LA-UR- 97-2474

Approved for public release; distribution is unlimited.

CONF-970727--

Title: New Paradigm for Simplified Combustion Modeling of Energetic Solids: Branched Chain Gas Reaction

Author(s): M.Q. Brewster, M.J. Ward, and S.F. Son

Submitted to: 33rd AIAA/ASME/SAE/ASEE Joint Propulsion Conference
July 6-9-, 1997
Seattle, WA

Los Alamos
NATIONAL LABORATORY

DISCLAIMER

AIAA 97-3333

New Paradigm for Simplified Combustion Modeling of Energetic Solids: Branched Chain Gas Reaction

M. Q. Brewster and M. J. Ward
University of Illinois at Urbana-Champaign
Urbana, IL

S. F. Son
Los Alamos National Laboratory
Los Alamos, NM

ABSTRACT

Two combustion models with simple but rational chemistry are compared: the classical high gas activation energy ($E_g/RT >> 1$) Denison-Baum-Williams (DBW) model, and a new low gas activation energy ($E_g/RT << 1$) model recently proposed by Ward, Son, and Brewster (WSB). Both models make the same simplifying assumptions of constant properties, Lewis number unity, single-step, second order gas phase reaction, and single-step, zero order, high activation energy condensed phase decomposition. The only difference is in the gas reaction activation energy E_g which is asymptotically large for DBW and vanishingly small for WSB. For realistic parameters the DBW model predicts a nearly constant temperature sensitivity σ_p and a pressure exponent n approaching 1. The WSB model predicts generally observed values of $n = 0.7$ to 0.9 and $\sigma_p(T_o,P)$ with the generally observed variations with temperature (increasing) and pressure (decreasing). The WSB temperature profile also matches measured profiles better. Comparisons with experimental data are made using HMX as an illustrative example (for which WSB predictions for $\sigma_p(T_o,P)$ are currently more accurate than even complex chemistry models). WSB has also shown good agreement with NC/NG double base propellant and HNF, suggesting that at the simplest level of combustion modeling, a vanishingly small gas activation energy is more realistic than an asymptotically large one. We conclude from this that the important (regression rate determining) gas reaction zone near the surface has more the character of chain branching than thermal decomposition.

A NEW PARADIGM FOR SIMPLIFIED COMBUSTION MODELING OF ENERGETIC SOLIDS: BRANCHED CHAIN GAS REACTION

M. Q. Brewster and M. J. Ward
University of Illinois at Urbana-Champaign
Urbana, IL

S. F. Son
Los Alamos National Laboratory
Los Alamos, NM

INTRODUCTION

For three decades the classical description of the gas phase reaction zone of burning energetic solids (at the simplest level of chemistry, i.e., single-step reaction) has been the high activation energy, flame sheet model $m \propto P^n \exp(-E_g / 2RT_f)$. This model first gained significant attention in 1961 with the pioneering paper of Denison and Baum[1]. In 1968 Culick[2,3] argued that it did not contain necessary coupling to the solid phase. However, in 1973 Williams[4] used activation energy asymptotics (AEA) analysis to show formally that such coupling was not warranted; in the limit of $E_g/RT >> 1$ the gas kinetics controlled expression of Denison and Baum was correct. (Numerical solution of the governing equations has since verified that for typical conditions of highly exothermic gas reaction and moderate, i.e., not low, pressure Williams was correct[5].) Nevertheless, the inability of the Denison/Baum/Williams (DBW) model to accurately predict certain important combustion parameters, such as pressure exponent and temperature sensitivity, was noted and various derivatives were developed in an attempt to couple the solid phase and better match experimental observations. Most of these models (such as BDP[6]) still retained the large E_g flame sheet assumption, or some manifestation of it. Some authors explored spatially distributed gas reaction descriptions, usually by assuming *a priori* the spatial distribution of heat release. None seems to have considered relaxing the large E_g assumption by formally considering the opposite limit.

In the time since the 1970s the trend in modeling has been toward development of more detailed chemical kinetic models. A consensus seems to have formed that any more accurate description of reality than $n = 1$ (for a single-step, bimolecular reaction) and $\sigma_p \approx$ constant should not be expected of a model as simple as single-step gas reaction. These limitations ($n = 1$ and $\sigma_p \approx c$) which are inherent in DBW have not been attributed to any erroneous assumption in the model (such as $E_g/RT >> 1$) but just the model's basic level of description, particularly the simplified chemistry. The assumption of large E_g itself seems to have been accepted. However, as more refined measurements of gas phase flame structure have become available recently and more computational studies conducted (much of this with double base NC/NG propellants), a curious result has emerged. The reported values of global gas activation energies seem to have reduced from the 40-50 kcal/mole range[6], for which analysis based on $E_g/RT >> 1$ is reasonably valid, to the range of 5-10 kcal/mole[7], where it is not. Yet, the simplified, single-step, level of description begun by Denison, Baum, and Williams for the limit of large E_g appears not to have been investigated for the opposite limit of small E_g until now.

A model which is the vanishingly small E_g analog of the DBW model has recently been developed by Ward, Son, and Brewster[8-10] (WSB). This exceedingly (perhaps deceptively) simple model demonstrates a surprising ability to accurately represent the essential features of energetic solid combustion. In this paper the derivation of the WSB model is given so that the common theoretical framework and assumptions it shares with the DBW model can be easily seen. Comparison is also made between the predictions of both models and HMX combustion data.

The overall objective of our work is to develop a reliable, predictive engineering model of combustion of energetic solids while developing new insight into basic combustion mechanisms. The approach is to use the simplest description which will include the essential physics and chemistry necessary to represent observable behavior. The observable behavior we are concerned with most is the macroscopic regression rate or mass flux, both steady and unsteady. To the degree that the temperature profile is important in determining regression rate (as is clearly the case via conductive heat feedback from the primary flame) we are also interested in its prediction (secondary flames are not of primary interest). Detailed species profiles are not of particular interest if simulating generic (i.e., reactant, intermediate, product) species can do the job of predicting regression rate. Observed behavior should be simulated to a degree that can establish confidence of predictive capability in untested situations. If

possible, blind testing of models should be done. As an example we present a comparison of model predictions with measured HMX combustion data. And as a test of predictive capability we present calculations of pressure-coupled response function, for which, to our knowledge, there are no measurements yet available.

THEORETICAL DESCRIPTION

The governing equations of the WSB model[8-10] are as follows. In the condensed phase an irreversible, unimolecular decomposition process is assumed,

$$A \rightarrow B \tag{1}$$

where A represents unreacted material, such as HMX, and B represents the decomposition products, such as NO_2, HONO, and larger fragments. Neglecting diffusion, the condensed phase species equation is

$$\rho_c \frac{\partial Y}{\partial t} + m\frac{\partial Y}{\partial x} = -\Omega_c;$$
$$Y(0,t) = 0; \quad Y(-\infty,t) = 1 \tag{2}$$

where Y represents the mass fraction of A. Consistent with Eqn. (1), a zero-order decomposition reaction is assumed.

$$\Omega_c = \rho_c A_c \exp\left[\frac{-E_c}{RT}\right] \tag{3}$$

The energy equation is

$$\rho_c C\frac{\partial T}{\partial t} + mC\frac{\partial T}{\partial x} = \lambda_c \frac{\partial^2 T}{\partial x^2} + Q_c\Omega_c$$
$$+qK_a \exp(K_a x);$$

$$T(0,t) = T_s; \quad T(-\infty) = T_o; \tag{4}$$

where in-depth absorption of radiant flux q has been allowed for. Conservation of mass (assuming constant density) relates the mass flux and regression rate as

$$m(t) = \rho_c r_b(t). \tag{5}$$

The steady state solution[11,12] for large activation energy ($E_c/RT >> 1$) and constant properties is

$$\frac{T(x) - T_o}{T_s - T_o} = \left[1 - \left(\frac{f_r J}{1-\beta}\right)\right]\exp\left(\frac{x}{x_c}\right)$$
$$+\left(\frac{f_r J}{1-\beta}\right)\exp\left(\frac{\beta x}{x_c}\right); \quad x<0 \tag{6}$$

$$r_b{}^2 = \frac{A_c\alpha_c \exp\left(\frac{-E_c}{RT_s}\right)}{\frac{E_c}{RT_s}\left(1-\frac{T_o}{T_s}\right)\left[1-\frac{\tilde{Q}_c}{2}-f_r J\right]}. \tag{7}$$

In the gas phase, an irreversible, bimolecular reaction is assumed,

$$B + M \rightarrow C + M \tag{8}$$

where B represents decomposition products, such as NO_2 and HONO, C represents intermediate gas phase products, such as NO, and M includes chain carriers such as N, H, OH, etc. For purposes of modeling species conservation, no distinction is made between the M species that appear on the left and right hand sides of Eqn. (8) although they would in general be different (i.e., unimolecular dissociation is not being implied). The process is assumed to be a bimolecular exchange reaction. The use of a common symbol M is an artifice of the simplified formulation, which for species bookkeeping purposes, assumes only two gas species, B (reactant) and C (product). The quasi-steady gas phase species equation, assuming Ficks law to represent upstream diffusion of C and downstream diffusion of B, is

$$m\frac{dY}{dx} = \rho_g D\frac{d^2Y}{dx^2} + -\Omega_g;$$
$$Y(0) = Y_s; \quad Y(\infty) = 0 \tag{9}$$

where Y represents mass fraction of B. Consistent with Eqn. (8), the following reaction rate is assumed, which is second order overall and first order with respect to reactant B

$$\Omega_g = B_g\rho_g^2 Y T^2 \exp(-E_g / RT)$$
$$= \left(B_g / (R/M)^2\right)P^2 Y \exp(-E_g / RT). \tag{10}$$

The T^2 term in the first prefactor allows for simple mathematical solutions. This is not in exact agreement with kinetic theory but is not a significant assumption in the present context since the assumed value of E_g is much more important with regard to the temperature dependence of the reaction rate. The quasi-steady gas phase energy equation is

$$mC\frac{\partial T}{\partial x} = \lambda_g \frac{\partial^2 T}{\partial x^2} + Q_g\Omega_g; \; T(0) = T_s; \tag{11}$$

$$T(\infty) = T_f = T_o + \left[Q_c + Q_g + q/m\right]/C.$$

Ideal gas behavior is assumed,

$$\rho_g = \frac{P}{(R/M)T}. \tag{12}$$

With the assumption of unity Lewis number ($\rho_g D = \lambda_g / C$= const) Eqs. (9) and (11) are equivalent and temperature and mass fraction are related by $Y=C(T_f-T)/Q_g$. The quasi-steady gas phase solution, assuming vanishingly small gas phase activation energy ($E_g = 0$) is [4]

$$\frac{T_f - T(x)}{T_f - T_s} = \frac{Y(x)}{Y_s} = \exp\left(-\frac{x}{x_g}\right);\ x>0 \tag{13}$$

$$x_g = \frac{2x_{cd}}{\sqrt{Da+1}-1} \tag{14}$$

$$Da = 4B_g\left(\frac{P}{R/M}\right)^2\left(\frac{C}{\lambda_g}\right)^2 x_{cd}^2 \tag{15}$$

$$x_{cd} = \frac{\rho_g D}{m} = \frac{\lambda_g}{mC} = \frac{\alpha_g}{u_g} \tag{16}$$

$$T_s = T_o + \frac{Q_c}{C} + \frac{1}{mC}\left[q + \frac{\lambda_g(T_f - T_s)}{x_g}\right]. \tag{17}$$

The steady regression rate or mass flux is obtained as an eigenvalue of the problem from Eqs. (7) and (14) through (17). Differentiating these equations, assuming constant Q_c and Q_g, gives the following temperature sensitivity ($\sigma_p = k/(T_s - T_o)$) and pressure exponent for the WSB model

$$k = \frac{1 + \dfrac{1}{\left(1-\dfrac{T_o}{T_s}\right)\left(1+\tilde{E}_c\right)\left(2-\tilde{Q}_c-2f_rJ\right)-1}}{\left\{\dfrac{2-\tilde{Q}_c-f_rJ}{\left(1-\dfrac{T_o}{T_s}\right)\left(1+\tilde{E}_c\right)\left(2-\tilde{Q}_c-2f_rJ\right)-1} + \dfrac{2\xi\tilde{Q}_g}{(1+\xi)(2+\xi)} + J\right\}} \tag{18}$$

$$n = \frac{\dfrac{2\xi\tilde{Q}_g}{(1+\xi)(2+\xi)}}{\left\{\dfrac{2-\tilde{Q}_c-f_rJ}{\left(1-\dfrac{T_o}{T_s}\right)\left(1+\tilde{E}_c\right)\left(2-\tilde{Q}_c-2f_rJ\right)-1} + \dfrac{2\xi\tilde{Q}_g}{(1+\xi)(2+\xi)} + J\right\}} \tag{19}$$

The formulation given above (for $E_g/RT \ll 1$) is the WSB model.

For comparison with the WSB model, the DBW solution as obtained by Williams[4,12] for the same assumptions (Le=1 and constant properties) except for $E_g/RT \gg 1$, is also considered. In this case an asymptotic series expansion for mass flux is obtained, which (to leading term only) is

$$m^2 = \frac{2\lambda_g B_g M^2 C T_f^4}{E_g^2 Q_g^2}\exp\left(\frac{-E_g}{RT_f}\right) \tag{20}$$

where T_f is as shown in Eq. (11). This expression indicates that mass flux is determined by gas kinetics only and not decomposition kinetics (unlike WSB where both gas and condensed phase chemistry play a role). The temperature and species profile is

$$\frac{T(x)-T_s}{T_f-T_s} = 1 - \frac{Y(x)}{Y_s} = \begin{cases} \dfrac{\exp(x/x_{cd})-1}{\exp(x_g/x_{cd})-1}; & 0<x<x_g \\ 1; & x>x_g \end{cases} \tag{21}$$

The convective-diffusive length scale x_{cd} is still defined by Eq. (16) but the flame location x_g is now given by an energy balance similar to Eq. (17) which can be written in the form

$$x_g = x_{cd}\ln\left[\frac{Q_g}{C(T_s-T_o)-Q_c-q/m}\right] \tag{22}$$

with T_s being determined by Eq. (7). Differentiating Eq. (20), assuming constant Q_g, gives the following temperature sensitivity ($\sigma_p = k/(T_s - T_o)$) and pressure exponent for the DBW model

$$k = \frac{2 + \tilde{E}_g}{\tilde{T}_f + J(2 + \tilde{E}_g)} \quad (23)$$

$$n = \frac{1}{1 + (2 + \tilde{E}_g)J / \tilde{T}_f}. \quad (24)$$

For negligible radiant flux ($J \rightarrow 0$) Eqs. (23) and (24) give

$$\sigma_p \rightarrow \frac{2 + E_g / 2RT_s}{T_o + \left(Q_c + Q_g\right)/C}; \quad n \rightarrow 1 \quad (25)$$

which predicts that the temperature sensitivity is independent of pressure, nearly independent of initial temperature (usually $T_o << \left(Q_c + Q_g\right)/C$; T_s is a very weak function of T_o), and strongly determined by the assumed value of E_g. To the degree the radiant flux is negligible, the pressure exponent approaches one. (In recognition of the latter difficulty most DBW derivatives[28] adopt an overall, non-integer gas reaction order less than 2.)

Numerical solution of the differential equations for arbitrary E_g has recently been done[5] and shown that the WSB and DBW analytic solutions are indeed correct for their respective limiting values of E_g for typical conditions of moderate (not subatmospheric) pressure and strongly exothermic gas flame.

RESULTS

The primary test conditions for model comparison are listed in Table 1, with simulation of HMX being considered as an example. Three pressures are considered, 1, 10, and 70 atm, with a laser flux of 35 W/cm^2 augmenting the combustion at 1 atm. At the two higher pressures combustion gas thermal radiation accounts for the assumed values of q. The value of E_c (42 kcal/mole) is close to the estimated bond strength of the N-NO_2 bond, rupture of which is thought to initiate decomposition. The absorption coefficient (5670 cm^{-1}) is for 10.6 μm (CO_2 laser) radiation (measured at room temperature using KBr-FTIR spectroscopy[13]) and is important for the 1 atm case only. For pressures above 2 atm, the prefactors A_c and B_g were determined by matching r_b (0.38 cm/s) and T_s (733 K) at 20 atm and 298 K. At 1 atm Q_g was decreased relative to the higher pressure cases (and B_g increased), based on the observation[14] that at 1 atm with laser radiation two distinct flames form with the primary flame reaching a plateau at 1300 to 1500 K; the secondary flame (unimportant for regression rate) is then formed far downstream.

The main results for the three primary cases are shown in Table 1. For each parameter there are two lines; the top line is the WSB result and the bottom is the DBW result. In the 1 atm case the surface regression is being driven to a large degree by the laser flux, as indicated by the relatively small value of the conductive heat feedback q_c compared to the absorbed radiant flux q, and the appreciable value of ν_q relative to ν (=n). For the 10 and 70 atm cases the combustion gas thermal radiation is not having a strong effect; conductive heat feedback is driving the regression, as indicated by small values of ν_q and the relatively large values of n. Most of the results listed in Table 1 are not remarkably different between the two models. However, one notable difference is that the DBW flame location x_g is much smaller than the characteristic (1/e) length scale x_g of the WSB flame for all three pressures. This is a direct result of the different E_g assumptions and is further discussed below with the temperature profiles. Another significant difference is in the values of n and σ_p at 10 and 70 atm. For DBW, n is close to one and σ_p is nearly constant. For WSB, n is closer to the observed values for HMX and σ_p shows a variation with pressure as discussed below. The Jacobian parameters (δ, n_s) are negative in consequence of the zero order, thermal decomposition process (see Appendix), as was first observed should be the case in 1995[15].

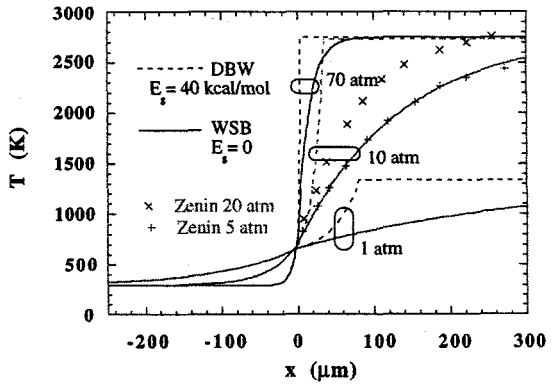

Fig. 1 Temperature profiles for HMX. Note similarity of gas profile shape between WSB model and Zenin[16] data.

Figure 1 shows the temperature profiles at 1, 10, and 70 atm. Both models have exponential temperature profiles, DBW concave-up and WSB concave-down. At the surface dT/dx is nearly the same for both models due to the regression rates being nearly the same. As pressure increases the response of the second order gas kinetics causes the

temperature profile to shift toward the surface. The question of how these predictions compare with measurements is important and needs careful consideration. Zenin has recently reported microthermocouple measurements for HMX[16] at 1, 5, 20 and 70 atm. These data show the same qualitative behavior as the WSB model, i.e., concave down. Zenin's 5 and 20 atm data are re-plotted in Fig. 1. The 5 atm Zenin data lie nearly on top of the 10 atm WSB model curve. By assuming that 10 atm measurements would fall halfway between the 5 and 20 atm data it can be seen that the WSB model at 10 atm underpredicts the thermocouple measurements somewhat, but is much closer qualitatively and quantitatively than the DBW model. The 1 atm WSB profile rises a little slower than Zenin's (not plotted) but the effect of laser augmentation would be to stretch the primary flame (Zenin's experiments had no laser augmentation) so that difference may be partly due to the radiant heat flux in the WSB 1 atm case. The 70 atm WSB profile rises faster than Zenin's (not plotted) but this may be partly due to thermocouple lag error which becomes more pronounced as pressure (regression rate) increases. The important result, however, is that the general shape of Zenin's measured temperature profiles is closer to that predicted by WSB than by DBW. Microthermocouple measurements in HMX have also been reported by Parr and Hanson-Parr at 1 atm with laser-augmentation[14]. These data appear similar to Zenin's except for a more pronounced initial concave-up curvature, which may be associated with a melt layer plateau or an effect of the laser augmentation used.

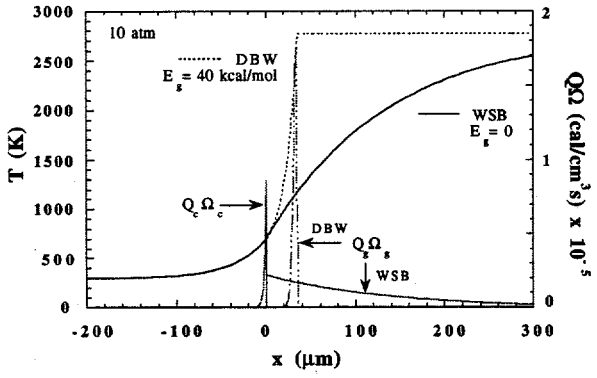

Fig. 2 Temperature profile and volumetric heat release at 10 atm for HMX.

Figure 2 shows the temperature profile again for the 10 atm case with the volumetric heat release rates due to chemical reaction ($Q_c\Omega_c$ and $Q_g\Omega_g$) added. In DBW the effect of large E_g is to concentrate all the gas phase heat release in a flame sheet. In WSB the effect of negligible E_g is to distribute the heat release broadly. Since these two models represent extreme (opposite) limiting conditions in terms of E_g, the actual heat release profile in a material such as HMX is probably an intermediate case between these two extremes. The experimental evidence of Fig. 1, however, suggests that the real case may be closer to the WSB limiting representation than DBW.

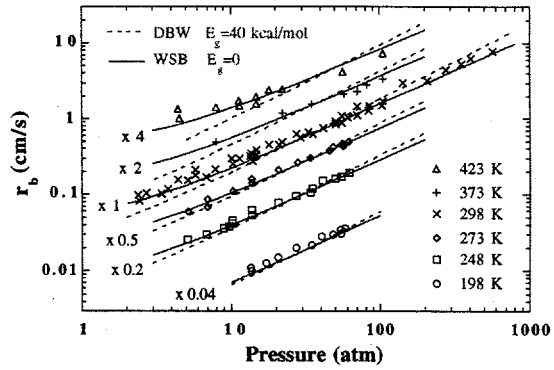

Fig. 3 Regression rate vs. pressure for HMX[17-19].

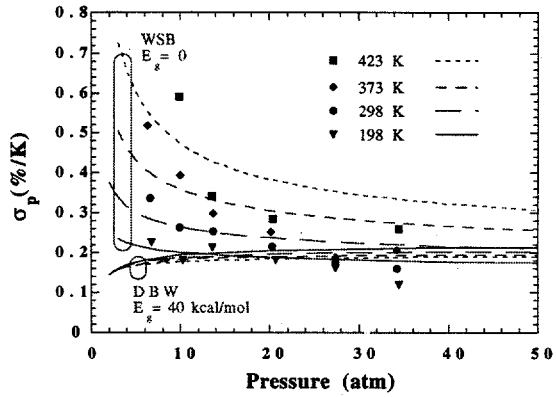

Fig. 4 Temperature sensitivity of regression rate for HMX[17-19].

The primary combustion parameter of interest in system design is the burning rate. Figure 3 show steady burning rate for HMX as a function of pressure for six initial temperatures, ranging from 198 K to 423 K, as obtained initially by Boggs[17,18] and later extended by Parr, et al.[19] The data above and below 298 K have a multiplier applied as shown to separate the data and make comparison with models easier. The fact that DBW inherently overpredicts the pressure exponent is evident in Fig. 3. WSB, however, naturally predicts the correct pressure exponent. The 423 K data also show that DBW underpredicts burn rate at low pressures and high temperatures. This shortcoming manifests itself in the temperature sensitivity, which is plotted in Fig. 4. The experimental data of Fig. 4 have been obtained from the Boggs/Parr data of Fig. 3 by curve-

fitting and analytically differentiating. This amplifies any error that may have existed in the original data. Nevertheless clear trends are evident showing that σ_p increases with temperature and decreases with pressure. These same observed trends are predicted by the WSB model, whereas the DBW model predicts σ_p is relatively independent of both pressure and temperature. Even the WSB model doesn't quite match experimental σ_p data in Fig. 4 as well as in Fig. 3, which is expected, Fig. 4 being the derivative. However, to put Fig. 4 in perspective it is important to realize that currently comprehensive HMX combustion models with hundreds of reactions cannot predict even the experimentally observed trends of $\sigma_p(T_o, p)$.

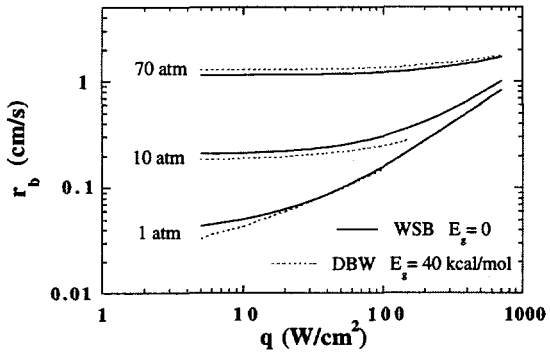

Fig. 5 Regression rate versus absorbed CO_2 laser flux for HMX.

Figure 5 shows model predictions of steady burning rate as a function of absorbed radiant flux for 1, 10, and 70 atm. The two models are not remarkably different except that DBW doesn't exhibit solutions for higher fluxes (above 100 W/cm^2) at lower pressures. (This is probably because Eq. (20) becomes invalid at low pressures and high radiant fluxes as discussed in Ref. 12 and the mass flux becomes determined by Eq. (7) with a zero temperature gradient condition imposed.) The results of Fig. 5 show that at a given pressure, say 10 atm, there is a cross-over radiant flux (about 100 W/cm^2 for 10 atm), below which conductive heat feedback becomes increasingly dominant (radiative feedback becoming negligible) and vice versa above. That cross-over flux increases with pressure due to the pressure-sensitive gas kinetics. One implication of this is that experiments that use laser energy to augment the combustion rate require a larger flux at higher pressures. Experimental verification of the results of Fig. 5 is being conducted in our laboratory. This requires measuring laser energy losses due to absorption and scattering in the combustion gas plume and reflection at the sample surface.

One example of a new experimental technique using laser energy to augment combustion is the laser-recoil method[20] for measuring the radiation driven burning rate response function R_q (see Appendix). Figure 6 shows the magnitude and phase of the laser-recoil response function for HMX at 1 atm at a mean CO_2 laser flux of 35 W/cm^2. Model predictions are for WSB (parameters in Table 1) and two independent experimental data sets[21,22] are shown. Figure 6 shows that the scaled magnitude data match reasonably well. With regard to the phase, Fig. 4 shows some variation between the two experimental data sets; however, the model values fall between the two measured data sets and exhibit the same trend with frequency. Underprediction of response phase at higher frequencies (approaching f_R) seems to be a characteristic of QS theory and probably is caused by violation of the QS assumption. Since the characteristic frequency of the condensed phase reaction layer is f_R=130 Hz, the QS phase would be expected to deviate as frequency approached this value. There may also be other factors affecting the applicability of the QS model to HMX combustion under these conditions. Perhaps complex, multiphase transport in the surface melt zone affects the response at these conditions, similar to what has been reported for RDX[23], but to a lesser extent. Nevertheless the degree of agreement is suggestive of a corresponding degree of accuracy in the model's representation of the actual complex combustion process. In particular, it is noteworthy that the decomposition energy barrier, 42 kcal/mole, corresponds to either of two competing initiation processes that might be expected for HMX decomposition, N-NO_2 bond scission and HONO elimination[24].

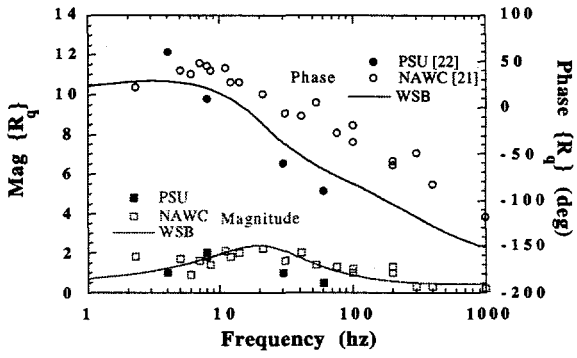

Fig. 6 Radiation-coupled response function for HMX (1 atm, 35 W/cm^2); QS theory and CO_2 laser-recoil measurements[21,22].

The greatest challenge for a combustion model is to simulate untested behavior. This is particularly

so for unsteady combustion. (Even with measurements available the track record for modeling unsteady combustion has not been very successful until recently with the replacement of the *ad hoc* Arrhenius surface pyrolysis relation Eq. (A1) with Eq. (7)[15].) A common unsteady performance measurement for energetic materials that appears not to have been reported yet for HMX is the pressure-coupled response function, R_p (see Appendix). T-burner tests of $Re\{R_p\}$ were planned for HMX sometime this year at China Lake. This situation offers a unique opportunity for double blind testing. The predicted pressure-coupled response for the parameters listed in Table 1 is shown in Fig. 7. The curves are only extended up to 300 hz at 10 atm and 5000 hz at 70 atm. We would expect the quasi-steady model to begin to fail at around these frequencies as the predicted decomposition layer response frequencies are f_R = 900 and 22,000 hz, respectively. The two models show similar behavior but with a reversal in pressure; the response is larger at 70 atm for DBW and slightly smaller for WSB. It will be interesting to see if future measurements correlate well with either of these or any model, including those with complex chemistry.

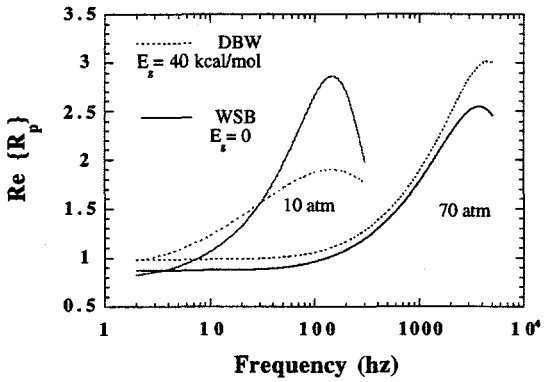

Fig. 7 Pressure-coupled response function for HMX; QS theory.

CONCLUDING REMARKS

The WSB model is the vanishingly small gas activation energy analog of the classical high activation energy single step gas reaction model of Denison and Baum and Williams (DBW). Whereas the regression rate in DBW is gas kinetically controlled, in WSB it is coupled to the condensed phase which is modeled as large activation energy decomposition. The WSB model is therefore a 2-step model with high activation energy decomposition in the condensed phase followed by vanishingly small energy barrier reaction in the gas phase. The decomposition is overall energetically neutral while the gas reaction is highly exothermic. The only difference between WSB and DBW is the value of E_g. The high E_g value of DBW results in a model which is essentially two thermal decomposition mechanisms in series, condensed phase thermal decomposition followed by gas phase thermal decomposition. In WSB the condensed phase process is the same (thermal) but the gas phase process, with negligible energy barrier (negligible temperature sensitivity), has more the character of a branched chain mechanism. The success of WSB in matching both temperature profile and burning rate behavior for HMX[8,10], NC/NG[9], and HNF[25] suggests that the latter description is closer to the actual case for many energetic materials. For complex chemistry combustion models to develop to the point of being able to predict $\sigma_p(T_o, p)$ accurately may require more attention to early gas phase branched chain chemistry, including decomposition species.

ACKNOWLEDGMENTS

The support of ONR (N00014-97-1-0085) and BMDO (N00014-95-1-1339) is gratefully acknowledged. The support of Los Alamos National Laboratory which is supported by the U. S. Department of Energy (W-7405-ENG-36) is also acknowledged. We would especially like to thank Drs. Richard S. Miller and Phil Howe for support and interest in this effort.

NOMENCLATURE

A_c = condensed phase reaction rate prefactor

A = $(T_s - T_o)(\partial \ln r_b/\partial T_s)_{p,q}$ (=k/r) or generic reactant species

B = $1/[(T_s - T_o)(\partial \ln r_b/\partial T_o)_{p,q}]$ (=1/k) or generic intermediate species

B_g = gas phase reaction rate prefactor

C = specific heat, C_p, or generic product species

D = binary diffusion coefficient in gas phase

Da = Damkohler number (gas phase)

E_c = activation energy of condensed phase

E_s = $E_c/2$

$\tilde{E}_c, \tilde{E}_g = E_c/2RT_s, E_g/2RT_f$

f = frequency (hz)

$f_{c,R} = 1/t_{c,R}$

f_r = $\exp(-K_a x_R)$, fraction of q absorbed below surface reaction zone

J = dimensionless mean radiant heat flux, $q/[mC(T_s-T_o)]$

K_a = absorption coefficient of condensed phase

k = $(T_s - T_o)(\partial \ln r_b/\partial T_o)_{p,q}$

M = molecular weight or generic chain carrier species

m = mass flux, $\rho_c r_b$

m' = $\Delta m \exp[i(2\pi ft+phase)]$

n_q = $(\partial \ln r_b/\partial \ln q)_{T_s,p}$ $(=\delta_q/r)$

n_s = $(\partial \ln \bar{r}_b/\partial \ln \bar{p})_{T_s,q}$ $(=\delta/r)$

n = $(\partial \ln \bar{r}_b/\partial \ln \bar{p})_{T_o,q}$ $(=\nu)$

P = pressure

P' = $\Delta P \exp[i2\pi ft]$

q = absorbed radiant heat flux in condensed phase

q_c = conductive heat flux to surface from gas phase

q' = $\Delta q \exp[i2\pi ft]$

$Q_{c,g}$ = heat release (positive exothermic)

$\tilde{Q}_{c,g}$ = $Q_{c,g}/C(T_s-T_o)$

QS = quasi-steady gas and condensed phase reaction zone assumption

R = universal gas constant, 1.987 cal/mole-K

R_p = pressure-driven frequency response function = $(m'/\bar{m})/(p'/\bar{p})$ at constant q

R_q = radiation-driven linear frequency response function = $(m'/\bar{m})/(q'/\bar{q})$ at constant p

r = $(\partial T_s/\partial T_o)_{p,q}$

r_b = burning rate

$t_{c,R}$ = characteristic times, $x_{c,R}/r_b$

$T_{o,s,f}$ = initial, surface, or final flame temperature

$\tilde{T}_f$ = $T_f/(T_s-T_o)$

x = coordinate normal to surface, positive into gas phase

x_c = solid convective-diffusive length scale, α_c/r_b

x_{cd} = convective-diffusive gas length scale, α_g/u_g

x_R = reaction zone length scale, $x_c/\tilde{E}_c$

x_g = gas flame characteristic thickness

Y = mass fraction of A (condensed) or B (gas)

$\alpha_{c,g}$ = thermal diffusivity

β = optical thickness (absorption only) of conduction zone ($K_a x_c$)

δ, δ_q = Jacobian parameters, $\nu r - \mu k$, $\nu_q r - \mu_q k$

Δ = amplitude of fluctuating quantity

λ = $1/2 + (1/2)(1 + 4i\Omega)^{1/2}$

$\lambda_{c,g}$ = thermal conductivity

μ = $[1/(T_s - T_o)](\partial T_s/\partial \ln p)_{T_o,q}$

μ_q = $[1/(T_s - T_o)](\partial T_s/\partial \ln q)_{T_o,p}$

ν = $(\partial \ln r_b/\partial \ln p)_{T_o,q}$ (same as n)

ν_q = $(\partial \ln r_b/\partial \ln q)_{T_o,p}$

$\rho_{c,g}$ = density

σ_p = $k/(T_s-T_o)$

ξ = x_g/x_{cd}

Ω = dimensionless frequency: $2\pi f \alpha_c/r_b^2$ or reaction rate

SUBSCRIPTS AND SUPERSCRIPTS

c = condensed phase, convective-diffusive, or conduction

cd = convective-diffusive (gas phase)

g = gas phase

r = radiation

R = reaction zone in condensed phase

s = surface

$\bar{}$ = steady condition or mean value

$\tilde{}$ = nondimensional quantity

$'$ = complex fluctuating quantity

REFERENCES

1. Denison, M. R. and E. Baum, "A simplified model of unstable burning in solid propellants," *ARS J.*, 31:1112-1122 (1961).

2. Culick, F. E. C., "A review of calculations for unsteady burning of a solid propellant," *AIAA J.*, 6, 2241-2255 (1968).

3. Culick, F. E. C., "An elementary calculation of the combustion of solid propellants," *Astr. Acta*, 14:171-181 (1969).

4. Williams, F. A., "Quasi-steady, gas-phase flame theory in unsteady burning of a homogeneous solid propellant," *AIAA J.*, 11:1328-1330 (1973).

5. Ward, M. J., "A simple model of steady combustion of HMX," M.S. thesis, University of Illinois, Urbana (1997).

6. Beckstead, M. W., "Model for double-base propellant combustion," *AIAA J.*, 18:980-985 (1980).

7. Lengelle, G., Bizot, A., Duterque, J., and Trubert, J. F., in *Prog. in Astro. and Aero.*, (K. K. Kuo and M. Summerfield, Eds.), AIAA, 90:389-393 (1984).

8. Ward, M. J., S. F. Son, and M. Q. Brewster, "A new paradigm in the simplest modeling of steadily burning HMX," 33rd JANNAF Combustion Meeting, CPIA Pub. 653, II:495-506 (1996).

9. Brewster, M. Q., M. J. Ward, and S. F. Son, "Unsteady combustion of homogeneous energetic solids," 33rd JANNAF Combustion Meeting, CPIA Pub. 653, II:181-192 (1996).

10. Ward, M. J., S. F. Son, and M. Q. Brewster, "Steady deflagration of HMX with simple kinetics: a new modeling paradigm," AIAA 97-0590, submitted to *Comb. Flame* (1997).

11. Lengelle, G., "Thermal degradation kinetics and surface pyrolysis of vinyl polymers," *AIAA J.*, 8:1989-98, (1970).

12. Ibiricu, M. W. and F. A. Williams, "Influence of externally applied thermal radiation on the burning rates of homogeneous solid propellants," *Comb. Flame*, 24:185-198 (1975).

13. Isbell, R. A. and M. Q. Brewster, "Optical properties of energetic materials: RDX, HMX, AP,

NC/NG, and HTPB," to appear, *Propellants, Explosives, and Pyrotechnics* (1998).
14. Parr, T. and D. Hanson-Parr, "Solid propellant flame chemistry and structure," in Non-Intrusive Combustion Diagnostics, K. K. Kuo and T. P. Parr eds., Begell House Inc., New York, 586 (1994).
15. Brewster, M. Q. and S. F. Son, "Quasi-steady combustion modeling of homogeneous solid propellants," *Comb. Flame,* 103:11-26 (1995).
16. Zenin, A., "HMX and RDX: combustion mechanism and influence on modern double-base propellant combustion," *J. Prop. Power*, 11:752-758 (1995).
17. Boggs, T. L., J. L. Eisel, C. F. Price, and D. E. Zurn, "High pressure burning rates of HMX," 15th JANNAF Combustion Meeting, CPIA Pub. 297, I:241-251 (1979).
18. Boggs, T. L., "The thermal behavior of RDX and HMX," in Fundamentals of Solid-Propellant Combustion, K. K. Kuo and M. Summerfield, eds., Prog. in Aero. Astro, AIAA, New York, 121-175 (1984).
19. Parr, T. P., T. L. Boggs, C. F. Price, and D. M. Hanson-Parr, "Measurement of the temperature sensitivies of ANAP-A and HMX burning rates," 19th JANNAF Combustion Meeting, CPIA, I:281-288 (1982).
20. Brewster, M. Q., Hites, M. H., and Son, S. F., "Dynamic burning rate measurements of metalized composite propellants using the laser-recoil technique," *Comb. Flame*, 94:178-190 (1993).
21. Finlinson, J. C., T. Parr, and D. Hanson-Parr, "Laser recoil, flame emission, and flame height combustion response of HMX and RDX at atmospheric pressure," 25th Symposium (International) on Combustion, The Combustion Institute, 1645-1650 (1994).
22. Litzinger, T. A., C. J. Tang, G. Kudra, and Y. J. Lee, "A study of the combustion response of the HMX monopropellant to sinusoidal laser heating," 33rd JANNAF Combustion Meeting, CPIA Pub. 653, II:159-168 (1996).
23. Brewster, M. Q. and T. B. Schroeder, "Unsteady combustion of homogeneous energetic solids," presented at the *Fourth International Symposium on Special Topics in Chemical Propulsion*, May 27-31, 1996, Stockholm, Sweden; to appear in symposium proceedings published by Begell House, Inc.
24. Naud, D. L. and K. R. Brower, "Pressure effects on the thermal decomposition of nitramines, nitrosamines, and nitrate esters," *J. Org. Chem.*, 57:3303-3308 (1992).
25. Louwers, J., G. M. H. J. L. Gadiot, M. Q. Brewster, S. F. Son, "A model for steady-state HNF combustion," International Workshop on Combustion Instability of Solid Propellants and Rocket Motors, Milano, Italy, 16-18, June, 1997.
26. Zebrowski, M. A. and M. Q. Brewster, "Theory of unsteady combustion of solids: investigation of quasi-steady assumption,"*J. Prop. Power*, 12:564-573 (1996).
27. Son, S. F. and M. Q. Brewster, "Linear burning rate dynamics of solids subjected to pressure or external radiant heat flux oscillations," *J. Prop. Power*, 9:222-232 (1993).
28. Mitani, T. and F. A. Williams, "A model for the deflagration of nitramines," 21st Symposium (International) on Combustion, The Combustion Institute, 1965-1974 (1986).

APPENDIX: QUASI-STEADY THEORY OF UNSTEADY COMBUSTION

For describing unsteady combustion, the classical theory of quasi-steady (QS) combustion of homogeneous energetic materials can be applied using the models outlined above, within certain limitations on frequency or time-constant of imposed changes. The QS theory is based on the assumption of quasi-steady reaction zones in *both* the gas and condensed phases. In the U.S. and Europe this theory (also called QSHOD for quasi-steady, homogeneous, one-dimensional) was developed in the context of the flame modeling (FM) approach whereas in the former Soviet Union the phenomenological Zeldovich-Novozhilov (ZN) approach was used. The two approaches are essentially equivalent. Within this common framework, thermal relaxation in the inert condensed phase, with time scale t_c, is the only non-quasi-steady process. The condensed phase reaction layer and the gas phase region are considered to respond instantly to changing external conditions. This formulation implicitly assumes that condensed phase reactions are confined to a thin region near the surface of the condensed phase (i.e., surface reaction) which is justified only if two conditions are met. First, the effective activation energy of the condensed phase decomposition must be large enough that a relatively thick inert convective-diffusive zone develops, followed by a thin reactive-diffusive zone ($E_c/RT \gg 1$; $x_c=\alpha_c/\bar{r}_b \gg x_R=x_c/(E_c/2RT_s)$). Typical values of $E_c/2RT_s$ for energetic materials are 5 to 15. For steady burning, even the smallest realistic values (~5) are large enough that AEA formulas (leading term only) such as Eq. (7) are accurate to within a few percent. This does not guarantee similar accuracy for oscillatory burning, however, which depends on the frequency of the imposed perturbation. Therefore, the second necessary condition is that the frequency of the perturbation be less than the characteristic frequency of the reaction layer ($f \ll f_R$)--how much less depends on the magnitude of $E_c/2RT_s$ and is something which has been only recently addressed[26]. Nevertheless it is to be expected that at some sufficiently large frequency

the QS model will fail by virtue of non-QS (i.e., distributed) reaction effects in the condensed phase, if not by some other mechanism.

While rigorous results for AEA-decomposition (e.g., Eq. (7)) have been available for many years they apparently have not been applied to unsteady combustion of solids until recently[15]. Instead, an *ad hoc* relation, usually referred to as Arrhenius surface pyrolysis,

$$r_b = A_s p^{n_s} q^{n_q} \exp(-E_s / RT_s) \qquad (A1)$$

has been almost universally assumed in FM studies, usually with n_s=0 and n_q=0. However, recent results for nitrate ester double base propellants[15] have shown that the simple but formally derived AEA formula based on single-step, zero order decomposition (Eqn. (7)) is superior to the Arrhenius surface pyrolysis formula for describing oscillatory burning. Therefore the formal AEA expression, Eqn. (7) has been incorporated in the WSB model instead of Eq. (A1).

In the linearized approximation the QS frequency response functions for pressure-perturbed burning (constant radiant flux) and radiation-perturbed burning (constant pressure) can be obtained[27] as

$$R_p = \frac{\nu + \delta(\lambda-1)}{\lambda r + k/\lambda - (r+k) + 1 - \dfrac{kf_r J(\lambda-1)}{\lambda(\beta+\lambda-1)}} = \frac{nAB + n_s(\lambda-1)}{\lambda + A/\lambda - (1+A) + AB - \dfrac{Af_r J(\lambda-1)}{\lambda(\beta+\lambda-1)}} \qquad (A2)$$

$$R_q = \frac{\nu_q + \delta_q(\lambda-1) - \dfrac{kf_r J(\lambda-1)}{\beta+\lambda-1}}{\lambda r + k/\lambda - (r+k) + 1 - \dfrac{kf_r J(\lambda-1)}{\lambda(\beta+\lambda-1)}} = \frac{\nu_q AB + n_q(\lambda-1) - \dfrac{Af_r J(\lambda-1)}{\beta+\lambda-1}}{\lambda + A/\lambda - (1+A) + AB - \dfrac{Af_r J(\lambda-1)}{\lambda(\beta+\lambda-1)}} \qquad (A3)$$

Equations (A2) and (A3) assume f_r (the surface reaction layer transmissivity) is a constant parameter. The steady state sensitivity parameters, k, r, ν, δ, ν_q, and δ_q are defined in the Nomenclature. The complete mathematical equivalence of the ZN and FM approaches at a term-by-term level (A=k/r, B=1/k, n=ν, n_s=δ/r, or n_q=δ_q/r), including the Jacobian parameters (n_s=δ/r, n_q=δ_q/r), was first demonstrated in 1993[27,15]. Before 1993 the equivalence of the n_s parameter appearing in the FM Arrhenius pyrolysis relation Eq. (A1) and the ZN Jacobian parameter δ had apparently not been recognized due to a subtle difference in linearization[27].

The steady state sensitivity parameters can either be obtained from experimental measurements of r_b and T_s while varying T_o, p, and q (ZN approach), or from flame modeling (FM). For the r- and μ- or δ-parameters the experimental approach has not proven to be sufficiently accurate. Therefore the FM approach is preferred for determining these parameters. By differentiating Eq. (7) relations for the r- and δ-parameters are obtained as follows, assuming constant Q_c.

$$r = \frac{k\left[2 - \tilde{Q}_c - f_r J\right] - 1}{\left(1 - \dfrac{T_o}{T_s}\right)\left(1 + \tilde{E}_c\right)\left(2 - \tilde{Q}_c - 2f_r J\right) - 1} \qquad (A4)$$

$$\delta = \frac{-\nu}{\left(1 - \dfrac{T_o}{T_s}\right)\left(1 + \tilde{E}_c\right)\left(2 - \tilde{Q}_c - 2f_r J\right) - 1} \qquad (A5)$$

$$\delta_q = \frac{-\nu_q + kf_r J}{\left(1 - \dfrac{T_o}{T_s}\right)\left(1 + \tilde{E}_c\right)\left(2 - \tilde{Q}_c - 2f_r J\right) - 1} \qquad (A6)$$

Equation (A5) shows that under normal circumstances (positive pressure exponent ν) the Jacobian parameters (δ, n_s) should be negative, as first reported in 1995[15].

The k- and ν-parameters are obtained by differentiating the complete set of equations which determine r_b and T_s. Assuming constant Q_c and Q_g, Eqs. (7) and (14) through (17) give, for the WSB model, Eqs. (18), (19), and

$$\nu_q = \frac{J + \dfrac{f_r J}{\left(1 - \dfrac{T_o}{T_s}\right)\left(1 + \tilde{E}_c\right)\left(2 - \tilde{Q}_c - 2f_r J\right) - 1}}{\left\{ \dfrac{2 - \tilde{Q}_c - f_r J}{\left(1 - \dfrac{T_o}{T_s}\right)\left(1 + \tilde{E}_c\right)\left(2 - \tilde{Q}_c - 2f_r J\right) - 1} + \dfrac{2\xi\tilde{Q}_g}{(1+\xi)(2+\xi)} + J \right\}} \qquad (A7)$$

while Eq. (20) gives, for the DBW model, Eqs. (23), (24), and

$$\nu_q = \frac{(2+\tilde{E}_g)J}{\tilde{T}_f + J(2+\tilde{E}_g)}. \qquad \text{(A8)}$$

Table 1. Material Properties and Combustion Parameters

P, atm		10	70	1 (with laser)
q, cal/cm^2-s		4.8	4.8	8.4
T_o, K		298	298	298
Condensed phase parameters				
ρ_c, g/cm^3		1.8	1.8	1.8
C, cal/g-K		0.335	0.335	0.335
α_c, cm^2/s		7.94e-4	7.94e-4	7.94e-4
E_c, kcal/mole		42.1	42.1	42.1
A_c, s^{-1}		9e15	9e15	9e15
Q_c, cal/g		60	60	40
K_a, cm^{-1}		5670	5670	5670
Gas phase parameters				
λ_g, cal/cm-s-K		1.67e-4	1.67e-4	1.67e-4
E_g, kcal/mole	WSB	0	0	0
	DBW	40	40	40
B_g, cal^2/atm^2-g-s-K^2-cm^3	WSB	2.22e-3	2.22e-3	3.50e-2
	DBW	4.20e2	4.20e2	3.47e7
$B_g P^2 M^2/R^2 \rho_g^*$ 1/s	WSB	1.95e4	1.39e5	1.77e4
	DBW	5.90e9	4.08e10	
Q_g, cal/g		758	758	250
T_f, K		2780	2750	1340
M, g/mole		24	24	24
Model Results				
T_s, K	WSB	705	793	663
	DBW	700	800	663
r_b, cm/s		0.22	1.15	0.080
		0.20	1.29	0.080
x_g, μm		135	15	315
		35	4	81
σ_p, K^{-1}		2.6e-3	2.0e-3	3.2e-3
		1.9e-3	2.0e-3	3.2e-3
q_c, cal/cm^2-s		26	215	3.5
		22	246	3.5
ν, n		0.79	0.88	0.36
		0.93	0.99	0.45
ν_q		0.089	0.014	0.52
		0.075	0.013	0.55
k		1.07	0.99	1.17
		0.75	1.02	1.16
r		0.050	0.046	0.065
		0.012	0.050	0.064
δ		-0.061	-0.065	-0.025
		-0.071	-0.073	-0.031
δ_q		-0.005	-0.0002	-0.035
		-0.005	-0.0002	-0.037
A		21	21	18

	63	20	18
B	0.93	1.0	0.85
	1.3	0.98	0.86
n_s	-1.2	-1.4	-0.38
	-5.1	-1.5	-0.48
n_q	-0.1	-0.004	-0.54
	-0.4	-0.004	-0.58

*based on $0.5(T_s+T_f)$ for WSB and T_f for DBW